Microbial Ecology (2021) 81:990–1003
https://doi.org/10.1007/s00248-020-01671-x

ENVIRONMENTAL MICROBIOLOGY

Nitrogen Assimilation Varies Among Clades of Nectar- and Insect-Associated Acinetobacters

Sergio Álvarez-Pérez[1,2] · Kaoru Tsuji[3] · Marion Donald[4] · Ado Van Assche[1] · Rachel L. Vannette[5] · Carlos M. Herrera[6] · Hans Jacquemyn[7] · Tadashi Fukami[8] · Bart Lievens[1]

Received: 15 June 2020 / Accepted: 20 December 2020 / Published online: 6 January 2021

Abstract

Floral nectar is commonly colonized by yeasts and bacteria, whose growth largely depends on their capacity to assimilate nutrient resources, withstand high osmotic pressures, and cope with unbalanced carbon-to-nitrogen ratios. Although the basis of the ecological success of these microbes in the harsh environment of nectar is still poorly understood, it is reasonable to assume that they are efficient nitrogen scavengers that can consume a wide range of nitrogen sources in nectar. Furthermore, it can be hypothesized that phylogenetically closely related strains have more similar phenotypic characteristics than distant relatives. We tested these hypotheses by investigating the growth performance on different nitrogen-rich substrates of a collection of 82 acinetobacters isolated from nectar and honeybees, representing members of five species (*Acinetobacter nectaris*, *A. boissieri*, *A. apis*, and the recently described taxa *A. bareti* and *A. pollinis*). We also analyzed possible links between growth performance and phylogenetic affiliation of the isolates, while taking into account their geographical origin. Results demonstrated that the studied isolates could utilize a wide variety of nitrogen sources, including common metabolic by-products of yeasts (e.g., ammonium and urea), and that phylogenetic relatedness was associated with the variation in nitrogen assimilation among the studied acinetobacters. Finally, nutrient source and the origin (sample type and country) of isolates also predicted the ability of the acinetobacters to assimilate nitrogen-rich compounds. Overall, these results demonstrate inter-clade variation in the potential of the acinetobacters as nitrogen scavengers and suggest that nutritional dependences might influence interactions between bacteria and yeasts in floral nectar.

Keywords *Acinetobacter* · Floral nectar · Insect · Nitrogen assimilation · Trait differentiation · Phylogenetic signal

Introduction

Floral nectar has traditionally been regarded as a mere sugar-rich reward that angiosperms offer to animals in return for their pollinating services [1, 2]. However, this canonical view of floral nectar as a sweet fluid mediating a bipartite relationship between pollinating animals and plants has been challenged in recent years. Nowadays, floral nectar is considered a complex solution of not only sugars but also proteins, amino acids, minerals, and other components (e.g., secondary

✉ Sergio Álvarez-Pérez
sergioaperez@ucm.es

✉ Bart Lievens
bart.lievens@kuleuven.be

[1] Department of Microbial and Molecular Systems, Laboratory for Process Microbial Ecology and Bioinspirational Management (PME&BIM), KU Leuven, B-3001 Leuven, Belgium

[2] Department of Animal Health, Complutense University of Madrid, 28040 Madrid, Spain

[3] Center for Ecological Research, Kyoto University, Hirano 2, Otsu, Shiga 520-2113, Japan

[4] Department of BioSciences, Rice University, Houston, TX 77005, USA

[5] Department of Entomology and Nematology, University of California Davis, Davis, CA 95616, USA

[6] Estación Biológica de Doñana, CSIC, 41092 Sevilla, Spain

[7] Biology Department, Laboratory of Plant Conservation and Population Biology, KU Leuven, B-3001 Leuven, Belgium

[8] Department of Biology, Stanford University, Stanford, CA 94305, USA

metabolites and volatile organic compounds) that can play many roles beyond pollinator attraction, including mediating interactions with herbivores, nectar robbers, and natural enemies [2–4]. Furthermore, floral nectar has been regarded as a short-lived, island-like habitat for diverse microorganisms (yeasts and bacteria in particular), which can alter nectar chemistry and affect plant-animal interactions in multiple ways [4–9]. Recent work has shown that flower visitors can influence the composition of nectar microbiota, by altering dispersal, growth, and long-term survival (e.g., between flowering seasons) of the microbial species [10–13].

Growth of microorganisms in floral nectar depends on their capacity to efficiently use the available nutrients and to tolerate the challenging conditions of nectar, including high osmotic pressures, unbalanced carbon-to-nitrogen ratios, diverse toxins of plant origin, and the fact that flowers are ephemeral habitats in which rapid growth is needed for population persistence [8, 9, 14–19]. For example, the chemical properties of floral nectar, especially carbon and nitrogen composition, vary between and within plant species [20–22], potentially shaping the spatial distribution of nectar microbes [18–23]. In particular, variation in the sugar concentration and composition among plants has been shown to contribute to maintaining spatial phenotypic variation in the nectar specialist yeasts *Metschnikowia reukaufii* and *M. gruessii* [18, 23]. Furthermore, nectar yeasts can use a variety of nitrogen sources and significantly decrease their concentration in floral nectar [24]. Genetic research has suggested that, through tandem duplications of genes involved in nitrogen metabolism and transport, nectar yeasts have evolved strategies to thrive in nitrogen-stressed environments like floral nectar and continue cell proliferation under conditions where other microbes perish [25]. However, how bacteria grow under these conditions remains largely unknown.

Members of the genus *Acinetobacter* (*Gammaproteobacteria*) rank among the most frequent bacterial inhabitants of floral nectar [6, 8, 26–29]. Acinetobacters isolated from nectar have also been found on pollinators and other flower visitors [11, 30]. The main nectar- and pollinator-associated acinetobacters identified so far include *Acinetobacter nectaris*, *A. boissieri*, *A. apis*, and the recently described species *A. pollinis*, *A. rathckei*, and *A. bareti* [28, 31] (Álvarez-Pérez S. et al., unpublished results). These species form a well-supported, deep-branching clade within the genus and are only capable of assimilating a limited selection of the main carbon sources available in floral nectar, including D-fructose in most cases and sucrose and D-glucose in some cases [28, 31, 32]. However, there is still limited information about the nitrogen assimilation capabilities of this bacterial group in nitrogen-poor environments such as floral nectar or the insect gut [15, 19, 33]. Furthermore, although in a previous study, we observed that phenotypic traits related to carbon assimilation and chemical sensitivity were linked to the phylogenetic placement of other *Acinetobacter* species [34], the phylogenetic and trait diversity of the nectar-and insect-inhabiting representatives are still poorly characterized [8, 28].

In this study, we investigated the nitrogen assimilation profiles of a diverse collection of acinetobacters isolated from nectar and honeybees, which can act as a vector of nectar microbes. Based on these profiles, we tested the hypotheses that (i) the studied isolates are capable of consuming a wide range of nitrogen sources, including those typically found in floral nectar and the insect digestive tract; and (ii) the phylogenetic affiliation of studied isolates was linked to their growth performance on different nitrogen-rich compounds, so that closely related lineages would phenotypically resemble each other more than distant relatives would. The effect of geographic origin, habitat (floral vs. insect), and specific microenvironments on nitrogen assimilation were also considered in these analyses.

Materials and Methods

Isolates

Eighty-two *Acinetobacter* isolates were analyzed in this study (Table S1). These isolates were isolated between 2011 and 2018 from different locations in the USA (42 isolates, 51%), Spain (20 isolates, 24%), Belgium (19 isolates, 23%), and Japan (1 isolate, 1%) from floral nectar and honeybees (*Apis mellifera*) (further referred to as "sample type"). Fifty-seven (70%) isolates originated from floral nectar of 16 different plant species, and 25 isolates (31%) had been obtained from the mouthparts, honey crop, or gut of honeybees (Table S1). All bacterial isolates were grown on trypticase soy agar (TSA; Merck Millipore, Overijse, Belgium) at 25 °C and stored at –80 °C in brain heart infusion (BHI) broth (Becton Dickinson, Erembodegem, Belgium) containing 25% glycerol (Merck Millipore) until further use. Identification of isolates as members of the genus *Acinetobacter* was based on some traits (Gram-negative, strictly aerobic, catalase-positive, and oxidase-negative coccobacilli [28, 35]) and the results of molecular-based methods (see Supplementary Methods).

Phylogenetic Reconstruction

Partial sequences of the gene encoding the β subunit of RNA polymerase (*rpoB*), which is a commonly used marker gene for assessing inter- and intra-species relationships of *Acinetobacter* members [36], were obtained as detailed in the Supplementary Methods and included in multiple alignments generated by MUSCLE [37]. The resulting alignments were trimmed with BioEdit v.7.0.9.0 [38] to ensure that all sequences had the same start and endpoint. Sequences differing in at least one nucleotide were classified into different

sequence types (STs) and a neighbor-joining (NJ) tree of STs was obtained using the maximum composite likelihood method, as implemented in MEGA X [39], and considering the *rpoB* gene sequence of *Acinetobacter calcoaceticus* NIPH 2245^T as an outgroup. The rate variation among sites was modeled with a gamma distribution, and support for the inferred topology was tested using 100 bootstrap replications. To provide solid evidence of the *rpoB*-based classification, additional phylogenetic trees were built by maximum likelihood (ML) and Bayesian inference (BI) approaches. The nucleotide sequences determined in this work have been deposited in the GenBank/ENA/DDBJ databases (see accession numbers in Table S1).

Nitrogen Assimilation Tests

The *Acinetobacter* isolates analyzed in this study were tested for their ability to assimilate 24 different nitrogen sources (Table S2, Fig. S1). These included nine protein amino acids (glycine, L-arginine, L-asparagine, L-cysteine, L-glutamic acid, L-histidine, L-leucine, L-proline, and L-tryptophan) and the non-protein amino acid L-ornithine, all of which are usually found in the floral nectar of diverse plant species [2, 22, 24, 40]. Other nitrogen sources tested in this study are usually included in the panels for metabolic analysis of *Acinetobacter* and other bacterial genera (e.g., [34, 41]). All assimilation tests were performed in 96-well assay plates, which were prepared as detailed in the Supplementary Methods.

Isolates from the −80 °C stock cultures were grown on TSA agar for 72 h at 25 °C, and then restreaked on TSA agar and incubated for 96 h at the same temperature. Next, cell suspensions were prepared by scraping bacterial colonies from the agar surface with a disposable loop (VWR, Oud-Heverlee, Belgium) and resuspending them in 10 mL of nitrogen-free basal mineral medium (BMM; see composition in the Supplementary Methods) to reach an optical density of 85%, as determined using a benchtop turbidimeter (Biolog, Hayward, CA, USA), which corresponds to a CFU count of $1.3\ 10^7 \pm 1.1\ 10^7$ CFU/mL (as determined using a selection of 10 *A. nectaris* and 5 *A. pollinis* isolates; no relevant differences in the CFU count was observed between these two species (Álvarez-Pérez S., unpublished data)). Then, bacterial cells were starved by incubating the cell suspensions in BMM inside an orbital shaker (150 rpm) at 25 °C for 4 h. Subsequently, each column of the assay plates was inoculated with 50 μL per well of a different strain (i.e., eleven isolates were tested per plate, and the twelfth column was left for cell-free sterility controls). Inoculated microplates were covered with a breathable membrane (Breath-Easy; Diversified Biotech, Boston, MA, USA). Final concentration of the tested compounds after adding the bacterial suspensions was 0.06% w/v in all cases, which corresponded with a nitrogen concentration ranging from 0.38×10^{-2} to 4.67×10^{-2} % w/v (mean ± SD = $1.28 \times 10^{-2} \pm 0.93 \times 10^{-2}$) (Table S2), whereas the sugars were at a concentration of 1% w/v (sucrose) or 0.1% w/v (glucose and fructose). The optical density (OD) at 600 nm of assay plates was measured using a benchtop spectrophotometer (Multiskan GO; Thermo Fisher, Merelbeke, Belgium) immediately after inoculation of bacterial cells (OD_0) and again after 96 h of static incubation at 25 °C (OD_f). At least three replicates for each isolate and test condition were run on different dates, and the order of isolates and cell-free controls in the columns of the plates was randomized in all cases. Additionally, some randomly chosen isolates were inoculated in two different columns of the same plate to test for intra-plate reproducibility of the assays.

Data Analysis

Performance of each isolate in a specific nitrogen assimilation test was assessed by determining the increase in the OD value obtained under that condition (i.e., $\Delta OD = OD_f - OD_0$), after subtracting the OD obtained in the negative control (which accounted for possible growth due to, for example, nutrient reserves remaining after the starvation step). Then, the average of the ΔOD values obtained for the replicates of each isolate and test condition was determined, and growth scores were calculated by dividing isolate-specific average ΔOD values by the maximum ΔOD obtained for all tested isolates in that particular assimilation assay. Furthermore, we calculated a nutrient assimilation (NA) index as the sum of the growth scores obtained for the assimilation of all nitrogen sources and which, therefore, gives an overall idea of the performance of isolates in the phenotypic tests considered in this study. The normal distribution of growth scores and the NA index was evaluated by the Shapiro-Wilk test, using the shapiro.test() function of R v. 3.6.1 package 'stats' [42].

Intra-plate reproducibility of the phenotypic assays was evaluated by calculating the concordance correlation coefficient (CCC) for agreement on continuous measures [43, 44], as implemented in the R library "epiR" (epi.ccc() function) [45]. Lin's CCC quantifies the agreement between two measures of the same variable and ranges from − 1 to 1, with perfect agreement at 1. In general, intra-plate reproducibility for testing assimilation of nitrogen compounds was good to excellent (the CCC 95% confidence intervals (CI) included values > 0.9 in 87.5% of the assimilation tests) (Table S3).

The distributions of growth scores obtained in each phenotypic test for the different *rpoB* clades and groups of isolates according to their geographical origin and sample type (floral nectar vs. insect) were visualized by beanplots [46], and pairwise correlations between traits were assessed by non-parametric Spearman rank tests, using the R package "Hmisc" [47]. In order to control for the non-phylogenetic independence of the isolates, correlation analyses were

repeated using phylogenetically independent contrasts (PICs) [48], as implemented in the R package "ape" (pic() function [49]). Phenotypic differences between groups of isolates according to their origin (sample type and geographic location) were analyzed by a phylogenetic ANOVA, which controlled for the non-independence of the data because of shared ancestry [50]. This latter test was carried out using the phylANOVA() function in the R package "phytools" [51]. In all cases, *P* values were adjusted for the number of simultaneous comparisons using Holm's correction.

Phylogenetic dependence of the phenotypic traits determined in this study was evaluated by calculating Blomberg's *K* and Pagel's λ [52–54], as implemented in the R packages "picante" (multiPhylosignal() function [55]) and "phytools" (phylosig() function), respectively. In both cases, the closer the value to zero, the more phylogenetically independent is a trait, while a value of 1 corresponds to a Brownian motion expectation (i.e., random walk with constant trait variance over time [48]), and values > 1 mean that close relatives are more similar than expected under Brownian motion [54, 56, 57]. Because some phylogenetic signal metrics are sensitive to polytomic branches [57], *K* and λ obtained for the whole data set (i.e., nitrogen assimilation and NA index data for all isolates, $n = 82$) were also compared to those obtained for a reduced data set that included the average growth scores and NA index obtained for each ST ($n = 32$, see below) in the different phenotypic tests. Relationships between pairwise phylogenetic distances and trait differentiation among isolates and STs were assessed by the Mantel test (mantel.test() function of the "ape" package), as detailed in Van Assche et al. [34]. In addition, we used the fitContinuous() function of R package "geiger" [58] to assess if the Brownian motion model of trait evolution actually provided a good fit to the phenotypic data or alternative models explained better trait evolution in the studied acinetobacters. The relative likelihood of different models was assessed by calculating their Akaike's information criterion (AIC) and Akaike weights [59], and when no evolutionary model showed an AIC weight ≥ 0.5, it was concluded that none of them performed substantially better than the others [34, 60]. The inputs of all these analyses were the NJ phylogenetic trees built from *rpoB* sequences (all sequences or a representative sequence of each ST) and converted into an ultrametric tree by using the force.ultrametric() function of "phytools," and the results obtained for nitrogen assimilation. Statistical significance was tested by randomization with 1000 repetitions and Holm-corrected *P* values < 0.05 were considered significant. Additionally, visualization of phenotypes on the NJ *rpoB* tree based on STs was achieved by using the phylo.heatmap() and contMap() functions of "phytools." In the contMap method, a color gradient is used to map observed and reconstructed trait values onto the edges of a phylogeny [61, 62].

Classic and phylogenetic principal component analysis (PCA) on the covariance matrices, as implemented in the R packages "stats" (princomp() function) and "phytools" (phyl.pca() function), respectively, were used to identify the test conditions accounting for most variability in the phenotypic data. PCA scree plots, loading plots, and scores plots were created using the R packages "graphics" and "ggplot2" [42, 63]. Additionally, permutational multivariate analysis of variance (PERMANOVA) was used to compare the growth performance of all the isolates in different test conditions, considering explanatory variables the nitrogen source, the *rpoB* clade and geographic origin (country) of the isolates, and the sample type from which these were obtained. These PERMANOVAs were carried out using the adonis() function of the R package "vegan" [64] and, given the high dimensionality of the data set, dissimilarity matrices between isolates were calculated based on the Manhattan distances using the vegdist() function of the same package.

Results

Partial sequencing of the *rpoB* gene revealed a total of 32 STs for the collection of isolates included in this study (Fig. 1, Table S1). The number of isolates of each ST ranged from one (in 19 STs, i.e., 59.4% of total) to 13 (one ST, ST14). Nineteen of those STs, comprising a total of 56 isolates, were identified as members of the species *A. nectaris* in BLASTn searches (98.1% to 100% sequence identity with the type strain). Five STs, representing a total of 14 isolates, formed a well-supported clade in the *rpoB* tree (> 90% bootstrap support and > 0.9 posterior probability in the NJ and BI analyses, respectively; Fig. 1, Figs. S2 to S4) and were identified as *A. pollinis* (99.8 to 100% sequence identity with the type strain). Five STs, comprising nine isolates, were identified as *A. boissieri* (99.3 to 99.9% identity with the type strain) and were closely related to the type strain of *A. bareti* (B10A^T) and a second isolate showing 99.7% identity to this type strain. Finally, a single ST containing just one isolate was identified as *A. apis* (99.8% sequence identity with the type strain).

The growth scores obtained in the 24 nitrogen assimilation assays and the NA index departed from normal distributions (corrected *P* values were < 0.05 in all cases). In general, results of nitrogen assimilation obtained for isolates from the different *rpoB* clades and groups of isolates according to their origin (sample type and geographic location) were broadly distributed, and the presence of outliers (i.e., isolates with a score which largely departed from the average for the clade/group) was a common finding for most nitrogen sources (see beanplots in Figs. S5–S7). NA indices were also broadly distributed across isolates from different *rpoB* clades, sample types, and geographical locations (Fig. S8). Correlation analysis of the growth scores and their corresponding PICs

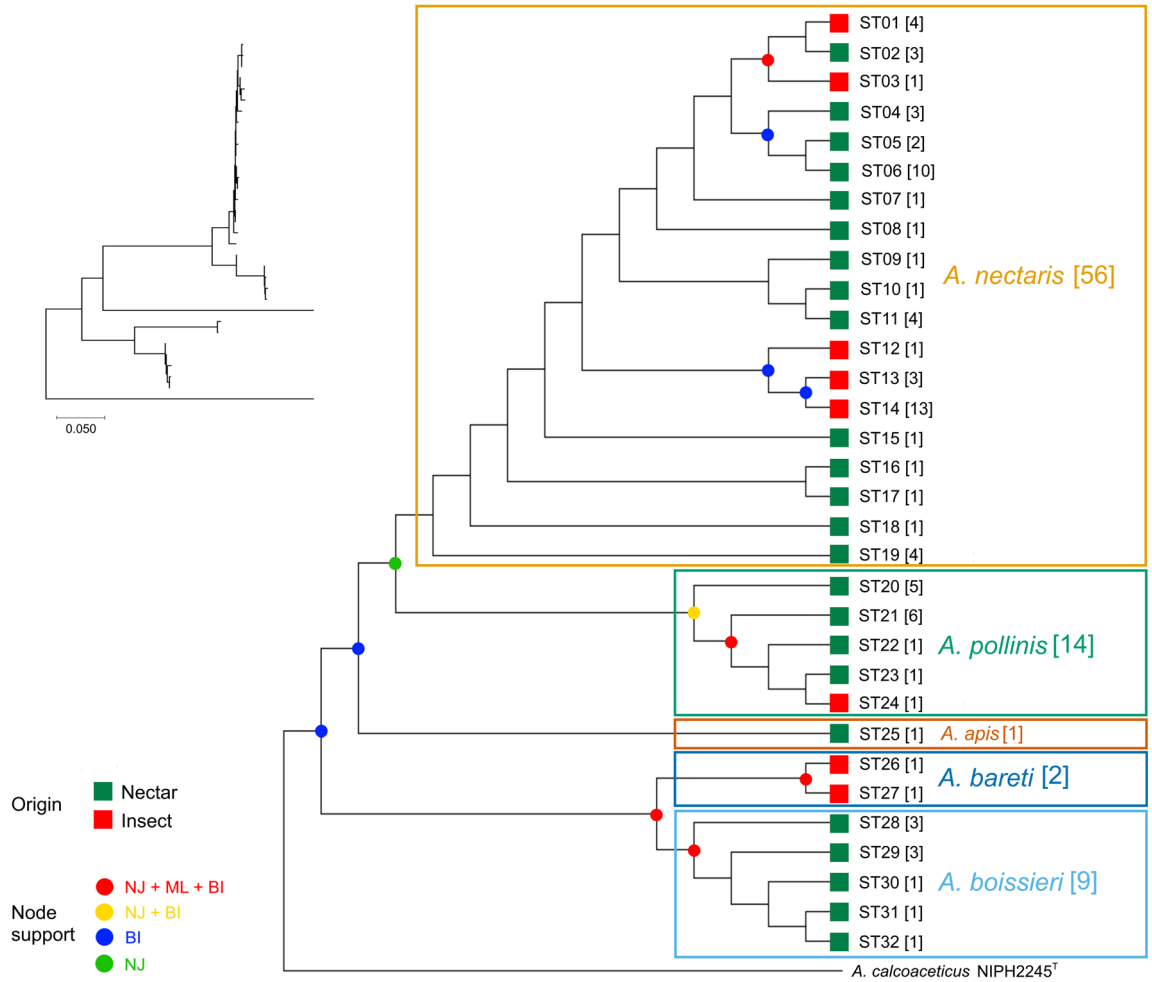

Fig. 1 Neighbor-joining (NJ) consensus tree, based on *rpoB* gene sequences, showing the relationships of the *Acinetobacter* isolates included in this study ($n = 82$). Branches correspond to the different *rpoB* sequence types (STs) identified based in nucleotide sequence alignments. The number of isolates belonging to each ST or species is indicated between square brackets. The small phylogram is included to illustrate branch length heterogeneity (see also Fig. S2). Evolutionary distances were computed using the maximum composite likelihood method and are in the units of number of base substitutions per site. The rate variation among sites was modeled with a gamma distribution. Alternative phylogenetic trees were obtained by maximum likelihood (ML) and Bayesian inference (BI) approaches (see details in the main text and Figs. S3 and S4). Node support values (bootstrap ≥ 90% based on 100 simulations for the NJ- and ML-based trees, and/or posterior probabilities ≥ 0.9 for the BI-based tree) are indicated by color-filled circles (see the legend at the lower left side of the figure). Color-filled squares on the tips of branches indicate the environmental origin of isolates (see the legend). GenBank accession numbers are given in Table S1. The tree was rooted with the *rpoB* gene sequence of *Acinetobacter calcoaceticus* NIPH 2245^T.

revealed 83 and 60 significant correlations between assimilation assays (30% and 21.7% of the total number of pairwise comparisons, $n = 276$), respectively, most of which (100% and 98.3%, respectively) were positive (Fig. S9). The only negative significant correlation corresponded to the PICs obtained for assimilation of nitrite and nicotinic acid ($\rho = -0.409$). In any case, Spearman's rank correlation coefficients were low for most trait pairs (absolute values of P were > 0.8 for only ten pairs of traits in the analysis based on growth scores and four pairs of traits when PICs were considered; Fig. S9).

The scores plot obtained by conventional and phylogenetic PCA of covariance matrices of nitrogen assimilation results are shown in Figs. 2 and 3, respectively, and the corresponding scree plots can be found in Fig. S10. The first two principal components explained 60.7% of the total variance in the conventional PCA and 70.2% in the phylogenetic PCA. The three variables with the highest contribution (i.e., the highest absolute value of loadings) to the first principal component in the conventional PCA were assimilation of L-asparagine (0.39), L-proline (0.37), and ammonium (0.37), whereas those with the greater influence on the second principal component were assimilation of uridine (− 0.47), L-histidine (− 0.44), and L-arginine (− 0.38) (Fig. 2 and S11). In contrast, assimilation of nitrite, betaine, and formamide had the greater influence on the first principal component of the phylogenetic PCA (loadings = − 0.99, − 0.99, and 0.61, respectively) (Fig. 3 and S11). Assimilation of L-glutamic acid,

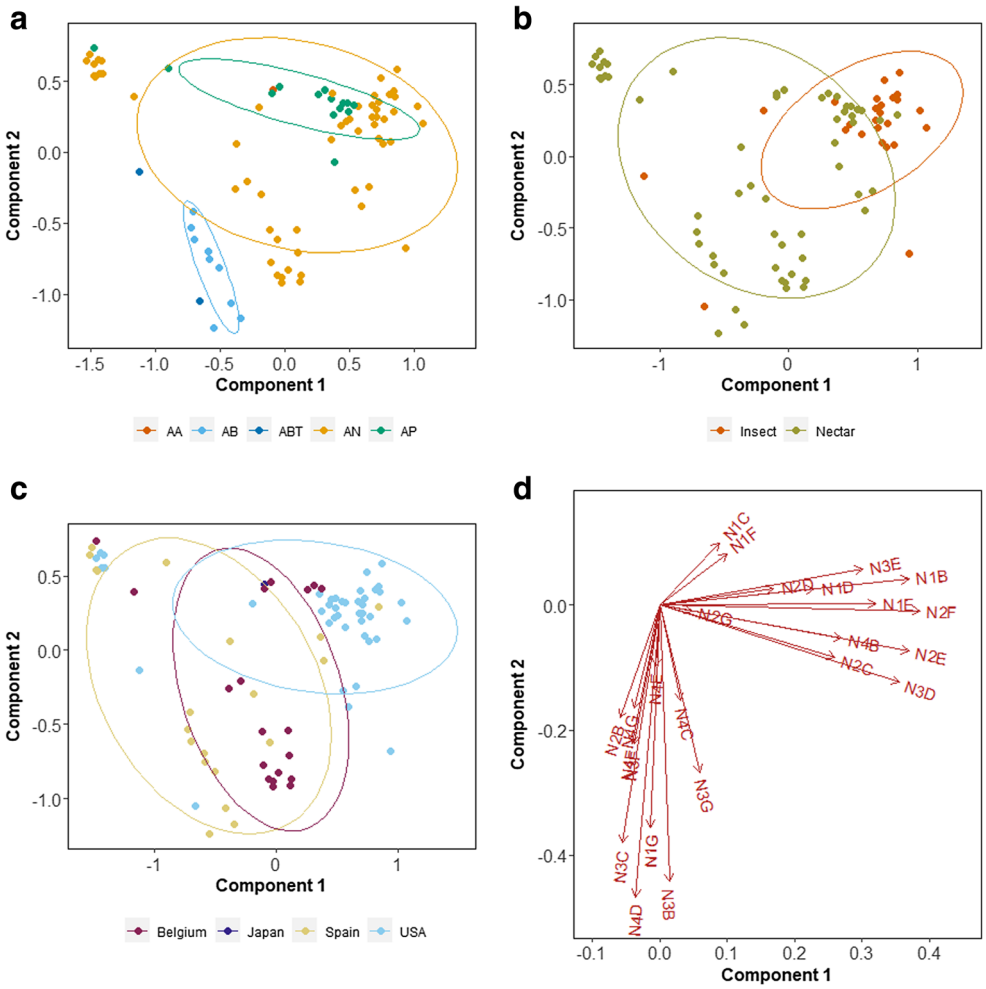

Fig. 2 **a**, **b**, and **c** Scores plots showing the distribution of *Acinetobacter* isolates according to the first two components obtained by conventional principal component analysis (PCA) of the covariance matrix of nitrogen assimilation data. Colors of points and the 68% data concentration ellipses denote different *rpoB* clades (panel **a**), sample sources (**b**) or countries of origin (**c**). **d** PCA loadings plot, where each arrow represents the loadings on the first two principal components for one factor (growth performance on a given nitrogen source). AA, *Acinetobacter apis* (n = 1); AB, *Acinetobacter boissieri* (n = 9); ABT, *Acinetobacter bareti* (n = 2); AN, *Acinetobacter nectaris* (n = 56); AP, *Acinetobacter pollinis* (n = 14). Codes of nitrogen assimilation tests are as in Table S2

L-proline, and uridine had the highest absolute loading values for the second principal component of the phylogenetic PCA (0.98, 0.97, and 0.96, respectively), but there were seven other variables with loadings > 0.8. The score plot obtained in the conventional PCA suggested phenotypic differentiation of the *A. bareti-A. boissieri rpoB* clade members, whereas the points representing the isolates of the other three species tested (*A. apis*, *A. nectaris*, and *A. pollinis*) were more intermingled and their corresponding 68% data concentration ellipses, which enclose approximately 2/3 of bivariate normal data, overlapped completely (Fig. 2). However, *rpoB* clade-based phenotypic differences were not supported by the phylogenetic PCA results (Fig. 3). Likewise, there was no clear grouping of isolates according to their origin, as isolates obtained from different sample types, geographic locations, and "microsites" (defined as different insect body parts or the floral nectar of different plant families) were intermingled in both the conventional and phylogenetic PCA scores plot (Figs. 2 and 3 and S12). Similar results were obtained when correlation matrices were used in the conventional and phylogenetic PCA (see Figs. S13 and S14, respectively); albeit in these cases, there was a clearer separation of the *A. bareti-A. boissieri rpoB* clades in the scores plot based on species identity.

Phylogenetic signal analysis based on the trait data obtained for the whole collection of *Acinetobacter* isolates (n = 82) yielded significant results for assimilation of most nitrogen sources when tested by Blomberg's and Pagel's method (19/24 and 18/24, i.e., 79.2% and 75%, respectively; Table 1). Accordingly, significant phylogenetic signal was also observed for the NA index ($P \leq 0.001$ in both methods). K values were in most cases low ($\leq 1.23 \cdot 10^{-7}$), indicating that the strength of phylogenetic signal was weaker than would be expected under a Brownian motion model. In contrast, high λ values (≥ 0.9) were obtained for 70.1% of the nitrogen assimilation assays and the NA index. Moreover, results of the Mantel test indicated that phylogenetic relatedness was associated with the observed variation in growth scores for most of the nitrogen sources tested (16/24, 66.7%) and the NA index (Table S4). Evolutionary model fitting of the whole data set indicated that the kappa model was the most commonly supported (87.5% of the assimilation assays and the NA index), followed by the white noise model (12.5%) (Table S5).

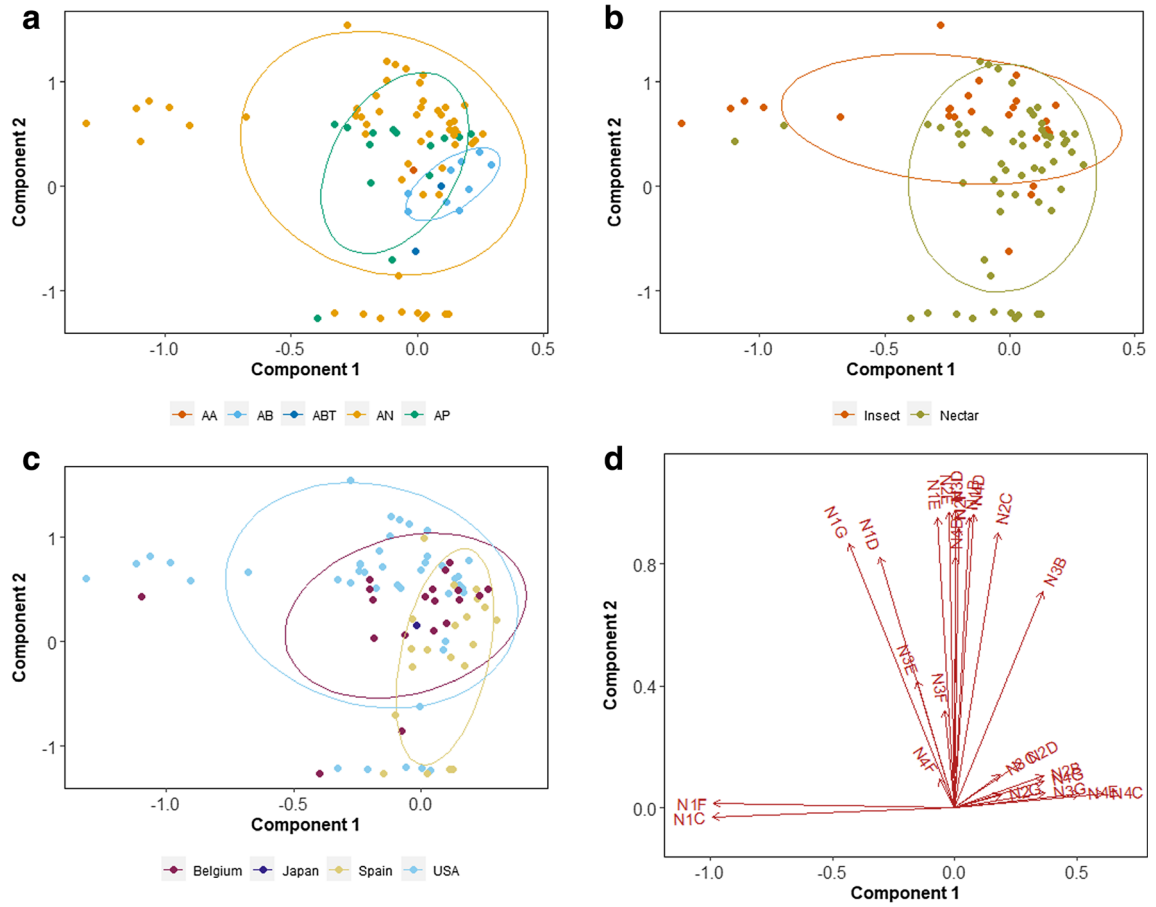

Fig. 3 **a**, **b**, and **c** Scores plots showing the distribution of *Acinetobacter* isolates according to the first two components obtained by phylogenetic principal component analysis (PCA) of the covariance matrix of nitrogen assimilation data. Colors of points and the 68% data concentration ellipses denote different *rpoB* clades (panel **a**), sample sources (**b**) or countries of origin (**c**). **d** Phylogenetic PCA loadings plot, where each arrow represents the loadings on the first two principal components for one factor (growth performance on a given nitrogen source). AA, *Acinetobacter apis* (n = 1); AB, *Acinetobacter boissieri* (n = 9); ABT, *Acinetobacter bareti* (n = 2); AN, *Acinetobacter nectaris* (n = 56); AP, *Acinetobacter pollinis* (n = 14). Codes of nitrogen assimilation tests are as in Table S2

A phylogenetic heatmap of the average growth scores obtained for the different *rpoB* STs in the nitrogen assimilation assays performed in this study is shown in Fig. 4, and the contMap trees mapping observed and estimated growth scores and NA indices onto the edges of the NJ tree built from STs can be found in Figs. S15 and S16, respectively. Repetition of the phylogenetic signal analysis using the average trait values of STs (reduced data set, n = 32) yielded significant results for assimilation of only six nitrogen sources (25%), namely glycine, L-arginine, glycyl-L-glutamic acid (Gly-Glu), and glycyl-L-aspartic acid (Gly-Asp) (significant results for both K and λ), L-tryptophan (only for K), and L-ornithine (only for λ) (Table 1, Fig. 4). Similarly, Mantel tests pointed to the phylogenetic dependence of the same six traits (Table S4). No significant phylogenetic signal was detected for assimilation of other nitrogen sources or the NA index. In addition, evolutionary model fitting of the reduced data set indicated that the white noise model was the most commonly supported (45.8% of the assimilation assays and the NA index), followed by the lambda and the kappa models (25% and 12.5%, respectively), and there were four traits (16.7%) for which no evolutionary model performed substantially better than the others (Table S6).

Phylogenetic ANOVAs using sample type and geographic origin of the isolates as factors revealed no significant difference between the groups considered for most nitrogen assimilation tests or the NA index (Table S7). The only two exceptions were the assimilation of the amino acids L-cysteine and L-tryptophan, for which significant differences were found between the nectar and insect isolates in the phylogenetic ANOVA (P = 0.046 and 0.024, respectively), with the insect isolates showing in general higher growth scores (see beanplots in Fig. S6). Furthermore, PERMANOVA analyses revealed that the performance of *Acinetobacter* isolates in the nitrogen assimilation assays depended significantly on the

Table 1 Phylogenetic signal of the growth performance of *Acinetobacter* isolates (n = 82) and *rpoB* sequence types (STs, n = 32) in nitrogen assimilation assays

Nitrogen assimilation test [code][a]	Phylogenetic signal metrics for isolates (P value[b])		Phylogenetic signal metrics for STs (P value[b])	
	Blomberg's K	Pagel's λ	Blomberg's K	Pagel's λ
Ammonium [N1B]	2.49E-08 (0.024*)	0.989 (< 0.001*)	2.59E-02 (0.195)	0.100 (1)
Nitrite [N1C]	2.20E-09 (1)	0.015 (1)	6.96E-03 (1)	0.059 (1)
Nitrate [N1D]	2.15E-08 (0.024*)	0.981 (< 0.001*)	3.14E-02 (0.204)	0.000 (1)
Urea [N1E]	3.15E-08 (0.024*)	0.989 (< 0.001*)	3.01E-02 (0.112)	0.000 (1)
Betaine [N1F]	2.14E-09 (1)	0.035 (1)	4.25E-03 (1)	0.030 (1)
Uracil [N1G]	3.70E-08 (0.024*)	0.997 (< 0.001*)	1.78E-02 (1)	0.188 (1)
Glycine [N2B]	2.35E-07 (0.024*)	0.754 (< 0.001*)	1.10E-01 (0.024*)	0.825 (< 0.001*)
L-Leucine [N2C]	4.92E-08 (0.024*)	0.995 (< 0.001*)	3.96E-02 (0.096)	0.000 (1)
L-Cysteine [N2D]	1.52E-08 (0.024*)	0.963 (< 0.001*)	3.93E-03 (1)	0.000 (1)
L(-)-Proline [N2E]	2.08E-08 (0.024*)	0.989 (< 0.001*)	2.70E-02 (0.096)	0.000 (1)
L-Asparagine [N2F]	1.76E-08 (0.024*)	0.985 (< 0.001*)	3.09E-02 (0.076)	0.213 (1)
N-Acetyl-D-glucosamine [N2G]	5.02E-09 (0.387)	0.000 (1)	6.44E-03 (1)	0.000 (1)
L-Histidine [N3B]	1.23E-07 (0.024*)	0.999 (< 0.001*)	3.17E-02 (0.090)	0.312 (1)
L-Arginine [N3C]	6.22E-08 (0.024*)	0.993 (< 0.001*)	7.00E-02 (0.024*)	0.764 (< 0.001*)
L-Glutamic acid [N3D]	2.28E-08 (0.024*)	0.992 (< 0.001*)	2.56E-02 (0.204)	0.000 (1)
L-Tryptophan [N3E]	1.73E-07 (0.024*)	0.999 (< 0.001*)	4.10E-02 (0.024*)	0.032 (1)
L-Ornithine [N3F]	8.93E-08 (0.024*)	0.930 (< 0.001*)	4.92E-02 (0.090)	0.920 (< 0.001*)
Glucosamine [N3G]	6.54E-09 (0.108)	0.000 (1)	2.24E-03 (1)	0.000 (1)
Ethanolamine [N4B]	2.43E-08 (0.024*)	0.995 (< 0.001*)	2.07E-02 (0.480)	0.000 (1)
Formamide [N4C]	1.32E-08 (0.024*)	0.792 (0.683)	1.24E-02 (1)	0.173 (1)
Uridine [N4D]	3.26E-08 (0.024*)	0.993 (< 0.001*)	2.54E-02 (0.250)	0.309 (1)
Nicotinic acid [N4E]	5.56E-08 (0.105)	0.223 (0.087)	5.10E-02 (0.432)	0.333 (0.853)
Gly-Glu [N4F]	8.57E-08 (0.024*)	0.998 (< 0.001*)	4.45E-02 (0.024*)	0.674 (0.001*)
Gly-Asp [N4G]	3.15E-07 (0.024*)	0.999 (< 0.001*)	9.53E-02 (0.024*)	0.855 (< 0.001*)
NA index[c]	2.19E-08 (0.001*)	0.989 (< 0.001*)	2.10E-02 (0.055)	0.000 (1)

[a] See details in Table S2

[b] Holm-corrected P values. Significant values (< 0.05) are denoted by an asterisk

[c] Nutrient assimilation index, defined as the sum of the growth scores obtained for the assimilation of all nitrogen sources

nitrogen source, the *rpoB* clade, the sample type, the geographical origin, all two-way interactions of these factors, and the three-way interaction between *rpoB* clade, geographical origin, and nitrogen source (Table 2).

Discussion

Recent research has revealed that carbon metabolism in bacteria follows some phylogenetic structure, and that this structure allows for some predictability in community assembly [34, 65, 66]. Although nitrogen is a major component of bacterial cells which accounts for 10–15% of their dry weight [67], there is still very limited information about the conservation and community ecology consequences of nitrogen metabolism.

The results of this study indicate that nectar- and pollinator-associated *Acinetobacter* clades differ in nitrogen assimilation capabilities. Moreover, as previously observed for nectar yeasts [18, 23, 68], we also found that phenotypic variation among the studied species was broad, with some outlying isolates of most species. Phylogenetic differences in assimilation of most individual nitrogen sources and the NA index, which was used as a measure of overall nitrogen assimilation, were confirmed by the results obtained for two different phylogenetic signal metrics (Blomberg's K and Pagel's λ) and Mantel tests using trait data for all isolates under study. However, there was some incongruence between the results obtained for Bloomberg's K and Pagel's λ, with most traits showing K values close to 0 but λ values close to 1. Unlike Blomberg's K, Pagel's λ is strongly robust to incomplete phylogenetic information (e.g., polytomies and non-accurate

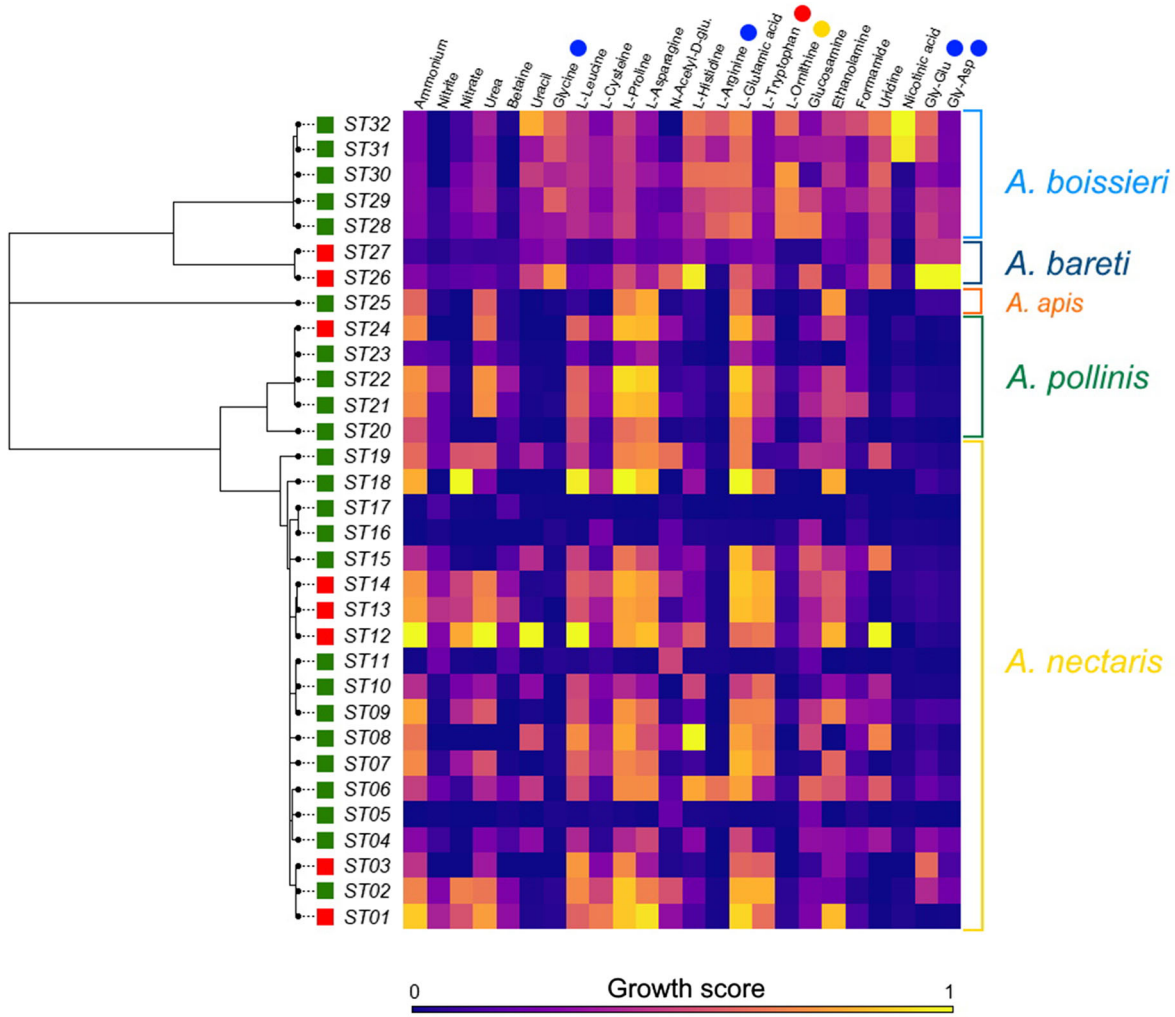

Fig. 4 Phylogenetic heatmap of the average growth scores obtained for the different *rpoB* sequence types (STs, shown in rows) in the nitrogen assimilation assays performed in this study (columns). The number of isolates belonging to each ST is indicated in Fig. 1. Color-filled squares on the tips of the phylogenetic tree indicate the environmental origin of isolates (green, floral nectar; red, insect). Phenotypes for which significant phylogenetic signal was detected when tested by Blomberg's *K*, Pagel's λ, or both methods are indicated by red, orange, and blue dots, respectively, next to the names of nitrogen sources

branch lengths) [57]. In our case, the original *rpoB* tree contained multiple polytomies that may contribute to the opposite trends observed for *K* and λ. Therefore, we recalculated the phylogenetic signal metrics using a reduced data set composed of the average trait values of STs. The results of this analysis showed a higher congruence between *K* and λ values and confirmed the significant phylogenetic dependence of assimilation of some amino acids typically encountered in floral nectar (glycine, L-arginine, L-tryptophan, and L-ornithine) and the dipeptides Gly-Glu and Gly-Asp, but not of the NA index. Moreover, contMap trees mapping observed and estimated growth scores and NA indices on the *rpoB* tree suggested a high conservation of trait values between closely related STs but a rapid loss of conservation deeper in the phylogeny (see Figs. S15 and S16), and model testing revealed that none of the studied traits followed a Brownian motion model of evolution, consistent with the results from a recent study on carbon assimilation of *Acinetobacter* species [34]. The kappa model, a punctuational model in which all branch lengths of the phylogenetic tree are raised to an estimated power (κ) and character divergence is related to the number of speciation events between two tips of the tree [52], fitted the results of most nitrogen assimilation assays and the NA index. In contrast, the white noise model, which assumes that trait data come from a random normal distribution and species have no significant trait covariance [60], fitted in most cases the average growth scores and NA indices calculated for STs. Nevertheless, variability in more than one-third of the average trait values of the STs (37.5%, including five of the six traits with significant phylogenetic signal) was better explained by more complex models of evolution, such as lambda (which fits the extent to which the phylogeny predicts covariance

Table 2 Output of the permutational multivariate analysis of variance (PERMANOVA) for the performance of *Acinetobacter* isolates in nitrogen assimilation assays[a]

Factors[b]	df	Sum Sqs	Mean Sqs	*F*	R^2	*P*
Clade	4	1.75	0.44	12.02	0.010	< 0.001#
Sample type	1	3.98	3.97	108.98	0.022	< 0.001#
Location	2	1.95	0.97	26.69	0.011	< 0.001#
N source	23	62.55	2.72	74.57	0.351	< 0.001#
Clade× Sample type	1	0.15	0.15	4.11	0.001	0.036#
Clade × Location	2	2.45	1.23	33.63	0.014	< 0.001#
Clade × N source	92	20.71	0.23	6.17	0.116	< 0.001#
Sample type × N source	23	12.17	0.53	14.51	0.068	< 0.001#
Location × N source	46	6.20	0.13	3.69	0.035	< 0.001#
Clade × Sample type × N source	23	0.62	0.03	0.73	0.003	0.856
Clade × Location × N source	46	3.50	0.08	2.09	0.020	< 0.001#
Residuals	1704	62.15	0.04	0.35		
Total	1967	178.17	1			

[a] The analysis was performed using the adonis() function of the R package vegan. *df* degrees of freedom, *Sum Sqs* sum of squares, *Mean Sqs* mean squares, *F F* statistics, R^2 partial *R*-squared, *P P* values based on 1000 permutations (statistically significant values are denoted by a hash symbol, #)

[b] Clade: *rpoB* clade; sample type: floral nectar vs. insect; location: country of origin (Belgium, Japan, Spain, or USA). *N source* nitrogen source (see Table S2)

among trait values for tips and transforms the tree by multiplying internal branches by λ [52]) and kappa.

Variation in microbial traits may also be linked to habitat differences, as different environmental conditions can select for different phenotypes. The PCA and the phylogenetic ANOVA results of this study mostly failed to detect significant correspondence between nutrient assimilation and sample type (floral nectar vs. honey bee) or the geographical origin of isolates. However, PERMANOVA results suggested that nitrogen assimilation depended not only on nutrient source and clade affiliation but also on the origin of isolates (sample type and/or country) and the interaction between origin and the aforementioned factors. Some of those interactions were expected as, for example, all *A. boissieri* isolates included in the assimilation tests had been retrieved from nectar samples collected in Spain, whereas the two *A. bareti* isolates were of insect origin and had been obtained in California, USA. Furthermore, the interaction between nitrogen sources and *rpoB* clade affiliation is another indication of the phylogenetic signal of nutrient assimilation observed in this and previous studies [34] for the members of genus *Acinetobacter*.

A methodological challenge that we had to face during the experimental part of this study was the preparation of cell suspensions from *Acinetobacter* plate cultures, due to the stickiness of the colonies of some isolates [8, 69, 70]. This trait may have contributed to the substantial variation in the CFU counts of the cell suspensions that we used to inoculate the assay plates. Additionally, as not all assimilation tests contained the same concentration of nitrogen and other nutrients (mostly carbon), the maximum growth possible in each source might vary and comparison of growth rates across tests should not be directly performed. To minimize the effect of these variations in the CFU counts and nitrogen content and allow a fairer comparison of the results obtained for different tests, we standardized the OD value obtained for each isolate in a given assimilation test with respect to maximum OD obtained in such a test. In any case, further refinement of the techniques used for phenotyping the nectar- and insect-associated acinetobacters is recommended.

The most common sources of nitrogen in nectar are the amino acids and proteins secreted by the plant and the nitrogen compounds released from pollen grains that fall into the nectary [15, 19, 22]. The frass of insects that visit flowers and the by-products of microbial metabolism can be additional sources of nitrogen in nectar. Although we did not analyze the chemical composition of the nectar samples from which our isolates were obtained, the data reported in previous studies suggest that the concentrations of some compounds that we used in our experiments are higher than those typically found in nature. For example, the concentration of different protein and non-protein amino acids in pristine nectar of *Diplacus aurantiacus* and the nectar of *Fritillaria lusitanica* (which are two of the plant species from which we obtained *Acinetobacter* isolates; Table S1), was found to range between 0 and 136 nmol/mL [24, 71]. These values are clearly below the amino acid concentrations that we used in our assays, which ranged between 2938 and 7993 nmol/mL. Nevertheless, as nectar chemistry can vary widely across plant species and even within a same species [22, 24, 40, 71, 72], it is difficult to reliably compare the nitrogen concentration in

our assimilation assays with that found in the floral nectar of the sampled species.

Our collection of *Acinetobacter* isolates mostly contained nectar isolates of *A. nectaris* (n = 34; i.e., 41.5% of the total number of isolates), followed by insect isolates of the same species (n = 22; 26.8%). Two of the species that we tested, *A. pollinis* and *A. bareti*, are still pending of formal description (Álvarez-Pérez S. et al., unpublished results), and there is not much information about their ecology or prevalence in nectar and insects, nor enough isolates available for a more balanced comparison with other species such as *A. nectaris* and *A. boissieri*. Similarly, there is still limited information about the ecology of *A. apis*, a species which was formally described by Kim et al. [31] but, to our knowledge, has never again been reported from any source until the present study. Unfortunately, due to the limited number of *Acinetobacter* isolates available for phenotyping in this study, our classification according to their origin only included very broad categories, such as "nectar" vs. "insect" or the country of sampling. Further classification of our collection of nectar isolates according to their plant host (at the family level) and the insect isolates according to their microsite of origin (mouth, crop, or gut) was attempted (see Fig. S12) and suggested no significant differentiation of isolates according to these criteria, but the number of isolates per category was too small to get reliable conclusions.

Acinetobacters frequently co-occur with other microorganisms in floral nectar, in particular with yeasts of the genus *Metschnikowia* [27]. In some cases, co-occurrence might be facilitated by resource partitioning between yeasts and bacteria in nectar as, for example, *Metschnikowia* spp. and the nectar acinetobacters have complementary nutrient assimilation profiles: the yeasts use glucose and enrich floral nectar in fructose, whereas the bacteria appear to preferentially use fructose [8, 28]. Furthermore, the results of the present study demonstrate that *Acinetobacter* isolates are capable of assimilating ammonium, urea, and different amino acids. These compounds are normally scarce in nectar, but may be supplemented through release of metabolic by-products by yeasts [73–75], diffusion from pollen grains that fall into nectar [19], and "directed bursting" of the fallen pollen grains by nectar yeasts [15]. However, because the common nectar yeast *M. reukaufii* is an efficient scavenger of scarce nitrogen [25, 76], it remains uncertain whether nitrogen released into nectar by yeasts can be taken up by bacteria or quickly scavenged by the yeasts themselves, leaving it possible that antagonistic competitive interactions are more prevalent than resource partitioning or facilitation among *Acinetobacter* and *Metschnikowia* spp. as their populations grow rapidly in nectar [76].

In general, bacteria use a large diversity of inorganic and organic compounds as sources of nitrogen [67]. However, as nitrogen assimilation can be energetically demanding, pathways for assimilation of nitrogen sources alternative to ammonium (which is generally the least expensive nitrogen source) are usually activated only when bacteria experience nitrogen deprivation [67]. Isolates from nitrogen-rich and nitrogen-poor habitats might therefore show differences in their nitrogen assimilation capabilities, with the latter being more efficient in nutrient scavenging. Furthermore, given the significant phylogenetic dependence of some phenotypes detected in this study, closely related species may display similar responses to variation in the nitrogen availability (overall concentration, diversity of available sources, etc.) in the environment. Unfortunately, the aforementioned limitations of our study precluded testing these hypotheses for the insect- and nectar-associated acinetobacters. Future research on this bacterial group should consider these and other unexplored potential sources of trait variation, including intra-species genetic diversity and epigenetic regulation, both of which appear to affect *Metschnikowia* yeasts in nectar [77, 78].

Conclusion

In conclusion, the results of this study demonstrate that the nectar- and insect-associated acinetobacters differ greatly in their assimilation of nitrogen sources and that phylogenetic relatedness predicts some of this variation in nitrogen assimilation. The results also suggest that nitrogen assimilation may depend on the origin (sample type and country) of isolates and the nutrient source. It remains to be determined, however, if isolates from nitrogen-rich and nitrogen-poor microsites (e.g., nectar types or body parts of insects) differ in their nitrogen assimilation patterns. Our results suggest that it would be interesting to study whether nutritional dependences facilitate or hinder co-occurrence of bacteria and yeasts in floral nectar and to what extent phenotypic variability in the acinetobacters increases spatial and temporal variation in the quality of nectar as a reward for pollinators.

Supplementary Information The online version contains supplementary material available at https://doi.org/10.1007/s00248-020-01671-x.

Acknowledgments We thank the members of KU Leuven's PME&BIM Lab and the Scientia Terrae Research Institute for feedback. The constructive comments from the journal's editor and four anonymous reviewers are gratefully acknowledged.

Authors' Contributions Conceptualization and resources: all authors. Investigation, formal analysis, and data curation: SA-P and AVA. Writing—original draft preparation: SA-P. Writing—review and editing: all authors. Supervision: BL and TF. Funding: SA-P, BL, and TF.

Funding This work was supported by funding from the European Union's Horizon 2020 research and innovation program (to SA-P, Marie Skłodowska-Curie Grant Agreement No. 742964) and the United States National Science Foundation (DEB 1737758). SA-P acknowledges a "Ramón y Cajal" contract funded by the Spanish Ministry of Science and Innovation [RYC2018-023847-I]. The funders had no role in the preparation of the manuscript or decision to publish.

Data Availability The nucleotide sequences determined in this work have been deposited in the GenBank/ENA/DDBJ databases under the accession numbers MN315286 to MN315354. All relevant results are included in this paper or available as supplementary materials at the journal's website.

Compliance with Ethical Standards

Conflict of Interest The authors declare that they have no conflict of interest.

Ethics Approval Ethics approval was not required.

Consent to Participate Not applicable.

Consent for Publication Not applicable.

References

1. Simpson BB, Neff JL (1981) Floral rewards: alternatives to pollen and nectar. Ann Missouri Bot Gard 68(2):301–322. https://doi.org/10.2307/2398800
2. Nepi M, Grasso DA, Mancuso S (2018) Nectar in plant-insect mutualistic relationships: from food reward to partner manipulation. Front Plant Sci 9:1063. https://doi.org/10.3389/fpls.2018.01063
3. Nepi M (2017) New perspectives in nectar evolution and ecology: simple alimentary reward or a complex multiorganism interaction? Acta Agrobot 70(1):1704. https://doi.org/10.5586/aa.1704
4. Parachnowitsch AL, Manson JS, Sletvold N (2019) Evolutionary ecology of nectar. Ann Bot 123(2):247–261. https://doi.org/10.1093/aob/mcy132
5. Belisle M, Peay KG, Fukami T (2012) Flowers as islands: spatial distribution of nectar-inhabiting microfungi among plants of *Mimulus aurantiacus*, a hummingbird-pollinated shrub. Microb Ecol 63(4):711–718. https://doi.org/10.1007/s00248-011-9975-8
6. Pozo MI, Lievens B, Jacquemyn H (2015) Impact of microorganisms on nectar chemistry, pollinator attraction and plant fitness. In: Peck RL (ed) Nectar: production, chemical composition and benefits to animals and plants. Nova Science Publishers Inc., New York, pp 1–40
7. Chappell CR, Fukami T (2018) Nectar yeasts: a natural microcosm for ecology. Yeast 35(6):417–423. https://doi.org/10.1002/yea.3311
8. Álvarez-Pérez S, Lievens B, Fukami T (2019) Yeast-bacterium interactions: the next frontier in nectar research. Trends Plant Sci 24(5):393–401. https://doi.org/10.1016/j.tplants.2019.01.012
9. Klaps J, Lievens B, Álvarez-Pérez S (2020) Towards a better understanding of the role of nectar-inhabiting yeasts in plant-animal interactions. Fungal Biol Biotechnol 7:1. https://doi.org/10.1186/s40694-019-0091-8
10. Hausmann SL, Tietjen B, Rillig MC (2017) Solving the puzzle of yeast survival in ephemeral nectar systems: exponential growth is not enough. FEMS Microbiol Ecol 93(12):fix150. https://doi.org/10.1093/femsec/fix150
11. Vannette RL, Fukami T (2017) Dispersal enhances beta diversity in nectar microbes. Ecol Lett 20(7):901–910. https://doi.org/10.1111/ele.12787
12. Pozo MI, Bartlewicz J, van Oystaeyen A, Benavente A, van Kemenade G, Wäckers F, Jacquemyn H (2018) Surviving in the absence of flowers: do nectar yeasts rely on overwintering bumblebee queens to complete their annual life cycle? FEMS Microbiol Ecol 94(12):fiy196. https://doi.org/10.1093/femsec/fiy196
13. Tsuji K, Fukami T (2018) Community-wide consequences of sexual dimorphism: evidence from nectar microbes in dioecious plants. Ecology 99(11):2476–2484 doi.org/10.1002/ecy.2494
14. Herrera CM, Canto A, Pozo MI, Bazaga P (2010) Inhospitable sweetness: nectar filtering of pollinator-borne inocula leads to impoverished, phylogenetically clustered yeast communities. Proc Biol Sci 277(1682):747–754. https://doi.org/10.1098/rspb.2009.1485
15. Herrera CM (2017) Scavengers that fit beneath a microscope lens. Ecology 98(10):2725–2726. https://doi.org/10.1002/ecy.1874
16. Lievens B, Hallsworth JE, Pozo MI, Ben Belgacem Z, Stevenson A, Willems KA, Jacquemyn H (2015) Microbiology of sugar-rich environments: diversity, ecology and system constraints. Environ Microbiol 17(2):278–298. https://doi.org/10.1111/1462-2920.12570
17. Pozo MI, Lachance MA, Herrera CM (2012) Nectar yeasts of two southern Spanish plants: the roles of immigration and physiological traits in community assembly. FEMS Microbiol Ecol 80(2):281–293. https://doi.org/10.1111/j.1574-6941.2011.01286.x
18. Pozo MI, Herrera CM, Van den Ende W, Verstrepen K, Lievens B, Jacquemyn H (2015) The impact of nectar chemical features on phenotypic variation in two related nectar yeasts. FEMS Microbiol Ecol 91(6):fiv055. https://doi.org/10.1093/femsec/fiv055
19. Pozo MI, Jacquemyn H (2019) Addition of pollen increases growth of nectar-living yeasts. FEMS Microbiol Lett 366(15):fnz191. https://doi.org/10.1093/femsle/fnz191
20. Herrera CM, Pérez R, Alonso C (2006) Extreme intraplant variation in nectar sugar composition in an insect-pollinated perennial herb. Am J Bot 93(4):575–581. https://doi.org/10.3732/ajb.93.4.575
21. Canto A, Pérez R, Medrano M, Castellanos MC, Herrera CM (2007) Intraplant variation in nectar sugar composition in two *Aquilegia* species (Ranunculaceae): contrasting patterns under field and greenhouse conditions. Ann Bot 99(4):653–660. https://doi.org/10.1093/aob/mcl291
22. Nicolson SW, Thornburg RW (2007) Nectar chemistry. In: Nicolson SW, Nepi M, Pacini E (eds) Nectaries and Nectar. Springer-Verlag, Dordrecht, pp 215–264
23. Pozo MI, Herrera CM, Lachance MA, Verstrepen K, Lievens B, Jacquemyn H (2016) Species coexistence in simple microbial communities: unravelling the phenotypic landscape of co-occurring *Metschnikowia* species in floral nectar. Environ Microbiol 18(6):1850–1862. https://doi.org/10.1111/1462-2920.13037
24. Peay KG, Belisle M (1729) Fukami T (2012) Phylogenetic relatedness predicts priority effects in nectar yeast communities. Proc Biol Sci 279:749–758. https://doi.org/10.1098/rspb.2011.1230
25. Dhami MK, Hartwig T, Fukami T (2016) Genetic basis of priority effects: insights from nectar yeast. Proc Biol Sci 283(1840):20161455. https://doi.org/10.1098/rspb.2016.1455
26. Fridman S, Izhaki I, Gerchman Y, Halpern M (2012) Bacterial communities in floral nectar. Environ Microbiol Rep 4(1):97–104. https://doi.org/10.1111/j.1758-2229.2011.00309.x
27. Álvarez-Pérez S, Herrera CM (2013) Composition, richness and nonrandom assembly of culturable bacterial-microfungal communities in floral nectar of Mediterranean plants. FEMS Microbiol Ecol 83(3):685–699. https://doi.org/10.1111/1574-6941.12027
28. Álvarez-Pérez S, Lievens B, Jacquemyn H, Herrera CM (2013) *Acinetobacter nectaris* sp. nov. and *Acinetobacter boissieri* sp.

nov., isolated from floral nectar of wild Mediterranean insect-pollinated plants. Int J Syst Evol Microbiol 63(Pt 4):1532–1539. https://doi.org/10.1099/ijs.0.043489-0
29. Sharaby Y, Rodríguez-Martínez S, Lalzar M, Halpern M, Izhaki I (2020) Geographic partitioning or environmental selection: what governs the global distribution of bacterial communities inhabiting floral nectar? Sci Total Environ 749:142305. https://doi.org/10.1016/j.scitotenv.2020.142305
30. Samuni-Blank M, Izhaki I, Laviad S, Bar-Massada A, Gerchman Y, Halpern M (2014) The role of abiotic environmental conditions and herbivory in shaping bacterial community composition in floral nectar. PLoS One 9(6):e99107. https://doi.org/10.1371/journal.pone.0099107
31. Kim PS, Shin NR, Kim JY, Yun JH, Hyun DW, Bae JW (2014) *Acinetobacter apis* sp. nov., isolated from the intestinal tract of a honey bee, *Apis mellifera*. J Microbiol 52(8):639–645. https://doi.org/10.1007/s12275-014-4078-0
32. Touchon M, Cury J, Yoon EJ, Krizova L, Cerqueira GC, Murphy C, Feldgarden M, Wortman J, Clermont D, Lambert T, Grillot-Courvalin C, Nemec A, Courvalin P, Rocha EPC (2014) The genomic diversification of the whole *Acinetobacter* genus: origins, mechanisms, and consequences. Genome Biol Evol 6(10):2866–2882. https://doi.org/10.1093/gbe/evu225
33. Engel P, Moran NA (2013) The gut microbiota of insects - diversity in structure and function. FEMS Microbiol Rev 37(5):699–735. https://doi.org/10.1111/1574-6976.12025
34. Van Assche A, Álvarez-Pérez S, de Breij A, De Brabanter J, Willems KA, Dijkshoorn L, Lievens B (2017) Phylogenetic signal in phenotypic traits related to carbon source assimilation and chemical sensitivity in *Acinetobacter* species. Appl Microbiol Biotechnol 101(1):367–379. https://doi.org/10.1007/s00253-016-7866-0
35. Cools P, Nemec A, Kämpfer VM (2019) *Acinetobacter*, *Chryseobacterium*, *Moraxella*, and other nonfermentative Gram-negative rods. In: Carroll KC, Pfaller MA, Landry ML, McAdam AJ, Patel R, Richter SS, Warnock DW (eds) Manual of Clinical Microbiology12th edn. ASM Press, Washington D.C., pp 829–857
36. La Scola B, Gundi VA, Khamis A, Raoult D (2006) Sequencing of the *rpoB* gene and flanking spacers for molecular identification of *Acinetobacter* species. J Clin Microbiol 44(3):827–832. https://doi.org/10.1128/JCM.44.3.827-832.2006
37. Edgar RC (2004) MUSCLE: multiple sequence alignment with high accuracy and high throughput. Nucleic Acids Res 32(5):1792–1797. https://doi.org/10.1093/nar/gkh340
38. Hall TA (1999) BioEdit: a user-friendly biological sequence alignment editor and analysis program for Windows 95/98/NT. Nucl Acids Symp Ser 41:95–98
39. Kumar S, Stecher G, Li M, Knyaz C, Tamura K (2018) MEGA X: molecular evolutionary genetics analysis across computing platforms. Mol Biol Evol 35(6):1547–1549. https://doi.org/10.1093/molbev/msy096
40. Petanidou T (2007) Ecological and evolutionary aspects of floral nectars in Mediterranean habitats. In: Nicolson SW, Nepi M, Pacini E (eds) Nectaries and Nectar. Springer-Verlag, Dordrecht, pp 343–375
41. Farrugia DN, Elbourne LD, Hassan KA, Eijkelkamp BA, Tetu SG, Brown MH, Shah BS, Peleg AY, Mabbutt BC, Paulsen IT (2013) The complete genome and phenome of a community-acquired *Acinetobacter baumannii*. PLoS One 8(3):e58628. https://doi.org/10.1371/journal.pone.0058628
42. R Core Team (2019) R: a language and environment for statistical computing. R Foundation for Statistical Computing, Vienna https://www.R-project.org/. Accessed 8 Apr 2020
43. Lin L (1989) A concordance correlation coefficient to evaluate reproducibility. Biometrics 45:255–268. https://doi.org/10.2307/2532051
44. Lin L (2000) A note on the concordance correlation coefficient. Biometrics 56:324–325
45. Stevenson M., Nunes T, Heuer C, Marshall J, Sanchez J, Thornton R, Reiczigel J, Robison-Cox J, Sebastiani P, Solymos P, Yoshida K, Jones G, Pirikahu S, Firestone S, Kyle R, Popp J, Jay M, Reynard C (2020) epiR: Tools for the analysis of epidemiological data. R package version 1.0-14. https://CRAN.R-project.org/package=epiR. Accessed 8 Apr 2020
46. Kampstra P (2008) Beanplot: a boxplot alternative for visual comparison of distributions. J Stat Softw 28:1–9. https://doi.org/10.18637/jss.v028.c01
47. Harrell FE, Dupont C, et al (2019) Hmisc: Harrell Miscellaneous. R package version 4.3-0. https://CRAN.R-project.org/package=Hmisc. Accessed 8 Apr 2020
48. Felsenstein J (1985) Phylogenies and the comparative method. Am Nat 125(1):1–15 www.jstor.org/stable/2461605
49. Paradis E, Claude J, Strimmer K (2004) APE: analyses of phylogenetics and evolution in R language. Bioinformatics 20:289–290. https://doi.org/10.1093/bioinformatics/btg412
50. Garland Jr T, Dickerman AW, Janis CM, Jones JA (1993) Phylogenetic analysis of covariance by computer simulation. Syst Biol 42(3):265–292. https://doi.org/10.1093/sysbio/42.3.265
51. Revell LJ (2012) Phytools: an R package for phylogenetic comparative biology (and other things). Methods Ecol Evol 3:217–223. https://doi.org/10.1111/j.2041-210X.2011.00169.x
52. Pagel M (1999) Inferring the historical patterns of biological evolution. Nature 401:877–884. https://doi.org/10.1038/44766
53. Blomberg SP, Garland Jr T, Ives AR (2003) Testing for phylogenetic signal in comparative data: behavioral traits are more labile. Evolution 57:717–745. https://doi.org/10.1111/j.0014-3820.2003.tb00285.x
54. Münkemüller T, Lavergne S, Bzeznik B, Dray S, Jombart T, Schiffers K, Thuiller W (2012) How to measure and test phylogenetic signal. Methods Ecol Evol 3:743–756. https://doi.org/10.1111/j.2041-210X.2012.00196.x
55. Kembel SW, Cowan PD, HelmusMR CWK, Morlon H, Ackerly DD, Blomberg SP, Webb CO (2010) Picante: R tools for integrating phylogenies and ecology. Bioinformatics 26:1463–1464. https://doi.org/10.1093/bioinformatics/btq166
56. Kamilar JM, Cooper N (2013) Phylogenetic signal in primate behaviour, ecology and life history. Phil Trans R Soc B 368:20120341. https://doi.org/10.1098/rstb.2012.0341
57. Molina-Venegas R, Rodríguez MA (2017) Revisiting phylogenetic signal; strong or negligible impacts of polytomies and branch length information? BMC Evol Biol 17(1):53. https://doi.org/10.1186/s12862-017-0898-y
58. Harmon LJ, Weir JT, Brock CD, Glor RE, Challenger W (2008) GEIGER: investigating evolutionary radiations. Bioinformatics 24:129–131. https://doi.org/10.1093/bioinformatics/btm538
59. Akaike H (1974) A new look at the statistical model identification. IEEE Trans Autom Control 19:716–723. https://doi.org/10.1109/TAC.1974.1100705
60. Narwani A, Alexandrou MA, Herrin J, Vouaux A, Zhou C, Oakley TH, Cardinale BJ (2015) Common ancestry is a poor predictor of competitive traits in freshwater green algae. PLoS One 10(9):e0137085. https://doi.org/10.1371/journal.pone.0137085
61. Revell LJ (2013) Two new graphical methods for mapping trait evolution on phylogenies. Methods Ecol Evol 4(8):754–759. https://doi.org/10.1111/2041-210X.12066
62. Revell LJ, Schliep K, Valderrama E, Richardson JE (2018) Graphs in phylogenetic comparative analysis: Anscombe's quartet revisited. Methods Ecol Evol 9(10):2145–2154. https://doi.org/10.1111/2041-210X.13067
63. Wickham H (2016) ggplot2: elegant graphics for data analysis. Springer-Verlag, New York

64. Oksanen J, Blanchet FG, Friendly M, Kindt R, Legendre P, McGlinn D, Minchin PR, O'Hara RB, Simpson GL, Solymos P, Stevens MHH, Szoecs E, Wagner H (2019) vegan: community ecology package. R package version 2.5-6. https://CRAN.R-project.org/package=vegan. Accessed 8 Apr 2020
65. Estrela S, Vila JCC, Lu N, Bajic D, Rebolleda-Gomez M, Chang C-Y, Sanchez A (2020) Metabolic rules of microbial community assembly. bioRxiv. https://doi.org/10.1101/2020.03.09.984278
66. Goldford JE, Lu N, Bajić D, Estrela S, Tikhonov M, Sanchez-Gorostiaga A, Segrè D, Mehta P, Sanchez A (2018) Emergent simplicity in microbial community assembly. Science 361(6401): 469–474. https://doi.org/10.1126/science.aat1168
67. Herrero A, Flores E, Imperial J (2019) Nitrogen assimilation in bacteria. In: Schmidt TM (ed) Encyclopedia of Microbiology4th edn. Academic Press, San Diego, pp 280–300
68. Dhami MK, Hartwig T, Letten AD, Banf M, Fukami T (2018) Genomic diversity of a nectar yeast clusters into metabolically, but not geographically, distinct lineages. Mol Ecol 27(8):2067–2076. https://doi.org/10.1111/mec.14535
69. Cooper RM, Tsimring L, Hasty J (2017) Inter-species population dynamics enhance microbial horizontal gene transfer and spread of antibiotic resistance. Elife 6:e25950. https://doi.org/10.7554/eLife.25950
70. Geisinger E, Isberg RR (2015) Antibiotic modulation of capsular exopolysaccharide and virulence in *Acinetobacter baumannii*. PLoS Pathog 11(2):e1004691. https://doi.org/10.1371/journal.ppat.1004691
71. Roguz K, Bajguz A, Chmur M, Gołębiewska A, Roguz A, Zych M (2019) Diversity of nectar amino acids in the *Fritillaria* (Liliaceae) genus: ecological and evolutionary implications. Sci Rep 9(1): 15209. https://doi.org/10.1038/s41598-019-51170-4
72. Vannette RL, Fukami T (2018) Contrasting effects of yeasts and bacteria on floral nectar traits. Ann Bot 121(7):1343–1349. https://doi.org/10.1093/aob/mcy032
73. Hess DC, Lu W, Rabinowitz JD, Botstein D (2006) Ammonium toxicity and potassium limitation in yeast. PLoS Biol 4(11):e351. https://doi.org/10.1371/journal.pbio.0040351
74. Ponomarova O, Gabrielli N, Sévin DC, Mülleder M, Zirngibl K, Bulyha K, Andrejev S, Kafkia E, Typas A, Sauer U, Ralser M, Patil KR (2017) Yeast creates a niche for symbiotic lactic acid bacteria through nitrogen overflow. Cell Syst 5(4):345–357.e6. https://doi.org/10.1016/j.cels.2017.09.002
75. Wu Q, Cui K, Lin J, Zhu Y, Xu Y (2017) Urea production by yeasts other than *Saccharomyces* in food fermentation. FEMS Yeast Res 17(7):fox072. https://doi.org/10.1093/femsyr/fox072
76. Tucker CM, Fukami T (2014) Environmental variability counteracts priority effects to facilitate species coexistence: evidence from nectar microbes. Proc Biol Sci 281(1778):20132637. https://doi.org/10.1098/rspb.2013.2637
77. Herrera CM, Pozo MI, Bazaga P (2012) Jack of all nectars, master of most: DNA methylation and the epigenetic basis of niche width in a flower-living yeast. Mol Ecol 21(11):2602–2616. https://doi.org/10.1111/j.1365-294X.2011.05402.x
78. Álvarez-Pérez S, Dhami MK, Pozo MI, Crauwels S, Verstrepen KJ, Herrera CM, Lievens B, Jacquemyn H (2021) Genetic admixture increases phenotypic diversity in the nectar yeast *Metschnikowia reukaufii*. Fungal Ecol 49:101016. https://doi.org/10.1016/j.funeco.2020.101016